December 2018

Microfluidic platforms for optical biosensing

Julie Lutti

Jing Wang

US010161853B1

(12) **United States Patent**
Lutti et al.

(10) **Patent No.: US 10,161,853 B1**
(45) **Date of Patent: *Dec. 25, 2018**

(54) **MICROFLUIDIC PLATFORMS FOR OPTICAL BIOSENSING**

(71) Applicant: **University of South Florida**, Tampa, FL (US)

(72) Inventors: **Julie Lutti**, St. Petersburg, FL (US); **Jing Wang**, Tampa, FL (US)

(73) Assignee: **University of South Florida**, Tampa, FL (US)

(*) Notice: Subject to any disclaimer, the term of this patent is extended or adjusted under 35 U.S.C. 154(b) by 0 days.

This patent is subject to a terminal disclaimer.

(21) Appl. No.: **15/475,874**

(22) Filed: **Mar. 31, 2017**

Related U.S. Application Data

(63) Continuation of application No. 14/181,149, filed on Feb. 14, 2014, now Pat. No. 9,687,847.

(60) Provisional application No. 61/764,298, filed on Feb. 13, 2013.

(51) **Int. Cl.**
G01N 15/14 (2006.01)
G01N 21/03 (2006.01)
G01N 21/05 (2006.01)

(52) **U.S. Cl.**
CPC ***G01N 21/05*** (2013.01); ***G01N 15/1484*** (2013.01); ***G01N 21/0303*** (2013.01); *G01N 2021/0346* (2013.01); *G01N 2201/0873* (2013.01)

(58) **Field of Classification Search**
CPC G01N 21/05; G01N 15/1484; G01N 21/0303; G01N 2201/0873; G01N 2021/0346; G01N 2021/058; G01N 21/7746; G01N 21/552; B01L 3/502761; B01L 2400/086; B01L 2300/0816; B01L 2200/0668; B01L 2300/0867
See application file for complete search history.

(56) **References Cited**

U.S. PATENT DOCUMENTS

6,583,399 B1 6/2003 Hunziker
6,879,752 B1 4/2005 Ilchenko et al.
7,259,855 B2 8/2007 Fan
2002/0114563 A1 8/2002 Tapalian
(Continued)

FOREIGN PATENT DOCUMENTS

WO 20100141365 A2 12/2010

OTHER PUBLICATIONS

Fan, et al., "Sensitive Optical Biosensors for Unlabeled Targets: A Review", ScienceDirect, Elsevier B. V., 2008, p. 8-26.
(Continued)

Primary Examiner — Lore R Jarrett
(74) *Attorney, Agent, or Firm* — Thomas | Horstemeyer, LLP

(57) **ABSTRACT**

In one embodiment, a microfluidic platform for optical biosensing, the platform including an optical substrate, a layer provided on the substrate, and a channel formed within the layer and defined by the layer and the substrate through which fluid can flow, the channel including a channel constriction that gradually narrows along a length of the channel to a point at which the channel is physically sized and configured to trap a microsphere suspended in the fluid when the fluid flows through the channel so that the microsphere cannot pass the channel constriction.

14 Claims, 5 Drawing Sheets

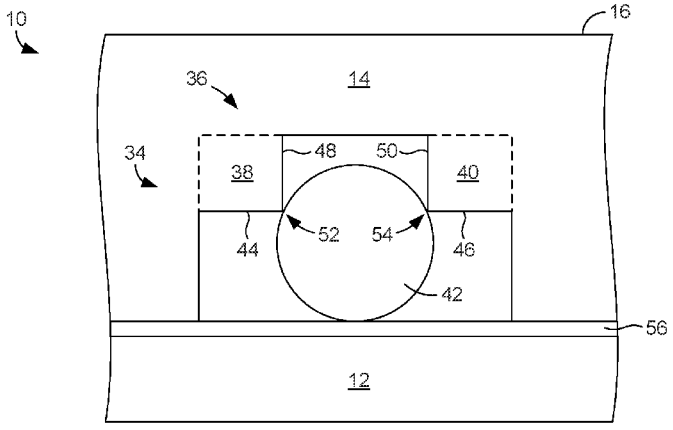

(56) **References Cited**

U.S. PATENT DOCUMENTS

2003/0174923	A1	9/2003	Arnold	
2004/0037739	A1*	2/2004	McNeely	B01F 5/10 422/417
2005/0077513	A1	4/2005	Fan	
2012/1019638		8/2012	Nitkowski	

OTHER PUBLICATIONS

Daria, et al., "Dynamic Formation of Optically Trapped Microstructure Arrays for Biosensor Applications", ScienceDirect, Elsevier B. V., 2004.

Bange, et al., "Microfluidic Immunosensor Systems", ScienceDirect, Elsevier B. V., Biosensors Biolectronics 20, 2005, pp. 2488-2503.

Lutti, et al. "A Monolithic Optical Sensor Based on Whispering-Gallery Modes in Polystyrene Microspheres", Applied Physics Letters 93, 2008.

Lutti, "High Q Optical Resonances of Polystyrene Microspheres in Water Controlled by Optical Tweezers", Applied Physics Letters 91, 2007.

Vollmer, et al., "Protein Detection by Optical Shift of a Resonant Microcavity", Applied Phys. Letter 80, 2002.

Abdelrahman, et al., Surface Functionalization Methods to Enhance Bioconjugation in Metal-Labeled Polystyrene Particles. Macromolecules, 2011. 44: p. 4801-4813.

Armani, et al., Ultra-Hihg-Q Microcavity operation in H[sub 2] O and D[sub 2]O. Applied Physics Letters, 2005. 87: p. 151118.

Amold, et al., "MicroParticle Photophysics Illuminates Viral Bio-Sensing", The Royal Society of Chemistry, 2008., 137.

Bierie, et al., "TGF-B and Cancer", Cytokine & Growth Factor Reviews, 2006, 17 (1-2): p. 29.40.

Chao, et al., "Polymer Microring Resonators for Biochemical Sensing Applications", IEEE Journal of Selected Topics in Quantum Electronics, 2006. 12(1): p. 134-412.

Chuang, et al., A Novel Fabrication Methods of Embedded Micro-Channels by Using SU-8 Thick-Film Photoresists. Sensors and Actuators a-Physical, 2003. 103 (1-2): p. 64-69.

Fan, et al., Sensitive Optical Biosensors for Unlabeled Targets: A Review: Analytica Chimica Acta, 2008, 620: p. 8-26.

Francois, et al., "Whispering Gallery Mode Biosensor Operating in the Stimulated Emission Regime", Applied Physics Letters, 2009. 94(3): p. 031101-3.

Gregor, et al., "An Alignment-Free Fiber-Coupled Microsphere Resonator for Gas Sensing Applications", Applied Physics Letters, 2010, 96: p. 231102.

Hanahan, et al., Hallmarks of Cancer: The Next Generation. Cell, 2011. 144(5), p. 646-674.

Heideman, et al. "Remote Opto-Chemical Sensing with Extreme Sensitivity: Design, fabrication and performance of a pigtailed integrated Optical Phase-Modulated Mach-Zehnder Interferometer System", Sensors and Actuators B-Chemical, 1999. 61(1-3): p. 100-127.

Hunt, et al. "Recycling Microcavity Optical Biosensors", Opt. Letter., 2011. 36(7): p. 1092-1094.

Ioppolo, et al., "Pressure Tuning of Whispering Gallery Mode Resonators", J. Opt. Soc. A. B, 2007. 24 (10): p. 2721-2726.

Knight, J.C., et al., Mapping Whispering-Gallery Modes in Microspheres with a near-Field Probe. Optics Letters, 1995.20(14): p. 1515-1517.

Lam, C.C., P.T. Leung, and K. Young, Explicit Asymptotic Formulas for the Positions, Widths, and Strengths of Resonances in Mie Scattering. Journal of the Optical Society of America B-Optical Physics, 1992. 9(9): p. 1585-1592.

Lee M.R. and P.M. Fauchet, Nanoscale microcavity sensor for single particle detection. Optics Letters, 2007. 32(22): p. 3284-3286.

Leosson, K. and B. Agnarsson, Integrated Biophotonics with CYTOP. Micromachines, 2012. 3(1): p. 114-125.

Li, H. and X. Fan, Characterization of sensing capability of optofluidic ring resonator biosensors. Applied Physics Letters, 2010. 97(1): p. 011105.

Lu, T., et al., High sensitivity nanoparticle detection using optical microcavities. Proceedings of the National Academy of Sciences of the United States of America, 2011. 108: p. 5976-5979.

Luppa P.B., L.J. Sokoll, and D.W. Chan, Immunosensors—principles and applications to clinical chemistry. Clinica Chimica Acta, 2001. 314(1-2): p. 1-26.

Senthil Murugan, G., et al., Position-dependent coupling between a channel waveguide and a distorted microsphere resonator. Journal of Applied Physics, 2010. 107: p. 053105.

Ong, B.H., X.C. Yuan, and S.C. Tjin, Adjustable refractive index modulation for a waveguide with SU-8 photoresist by dual-UV exposure lithography. Applied Optics, 2006. 45(31): p. 8036-8039.

Shera, E.B., et al., Detection of Single Fluorescent Molecules. Chemical Physics Letters, 1990. 174(6): p. 553-557.

Shew, B.Y., et al., UV-LIGA interferometer biosensor based on the SU-8 optical waveguide. Sensors and Actuators a-Physical, 2005. 120(2): p. 383-389.

Shopova, S.I., et al., Ultrasensitive nanoparticle detection using a portable whispering gallery mode biosensor driven by a periodically poled lithium-niobate frequency doubled distributed feedback laser. The Review of scientific instruments, 2010. 81: p. 103110.

Sunkara, V., et al., Simple room temperature bonding of thermoplastics and poly(dimethylsiloxane). Lab on a Chip, 2011. 11(5): p. 962-965.

Teraoka, I., S. Arnold, and F. Vollmer, Perturbation approach to resonance shifts of whisperinggallery modes in a dielectric microsphere as a probe of a surrounding medium. Journal of the Optical Society of America B-Optical Physics, 2003. 20(9): p. 1937-1946.

Tong, L.M., et al., Self-modulated taper drawing of silica nanowires. Nanotechnology, 2005. 16(9): p. 1445-1448.

Vlachopoulou, M.E., et al., A low temperature surface modification assisted method for bonding plastic substrates. Journal of Micromechanics and Microengineering, 2009. 19(1).

Vollmer, F., S. Arnold, and D. Keng, Single virus detection from the reactive shift of a whisperinggallery mode. Proceedings of the National Academy of Sciences of the United States of America, 2008. 105(52): p. 20701-4.

Vollmer, F., et al., Protein detection by optical shift of a resonant microcavity. Applied Physics Letters, 2002. 80(21): p. 4057-4059.

Wang, S., et al., Label-free imaging, detection, and mass measurement of single viruses by surface plasmon resonance. Proceedings of the National Academy of Sciences of the United States of America, 2010. 107(37): p. 16028-32.

Ymeti, A., et al., Fast, ultrasensitive virus detection using a young interferometer sensor. Nano Letters, 2007. 7(2): p. 394-397.

Wilson, et al. Whispering Gallery Mode Biosensor Quantification of Fibronectin Adsorption Kinetics onto Alkylsilane Monolayers and Interpretration of Resultant Cellular Response, Biomaterials 33 (2012) 225-236.

Soteropulos, et al., Determination of Binding Kinetics Using Whispering Gallery Mode Microcavities. Applied Physics Letters 99, 2011.

Schneider, et al., Hartman Interferometer: Versatile Integrated Optic Sensor for Label-Free, Real-Time Quantification of Nucleic Acids, Proteins, and Pathogens. Clinical Chemistry, 1757-1763, 1997.

Nordstrom, et al., Single-Mode Waveguides with SU-8Polymer Core and Cladding for MOEMS Applications. Journal of Lightwave Technology, vol. 25, No. 5, May 2007.

Nadeau, et al., High-Q Whispering-Gallery Mode Sensor in Liquids. Jet Propulsion Laboratory, 2002.

Mott, et al., The Bulk Modulus and Poisson's Ratio of "Incompressible" Materials. Science Direct, Journal of Sound and Vibration, 2008.

* cited by examiner

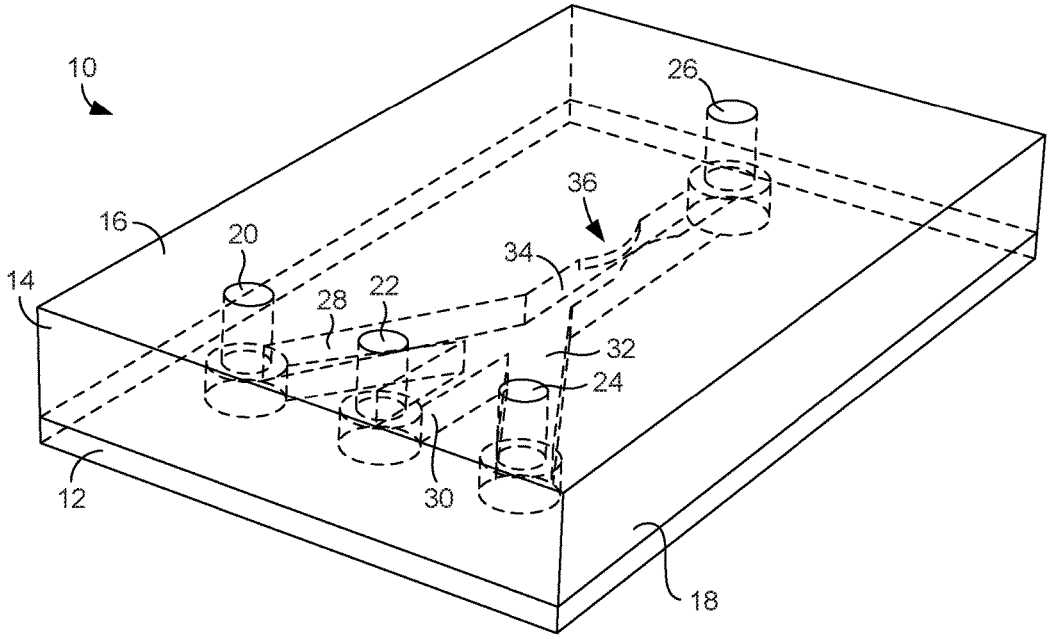

FIG. 1

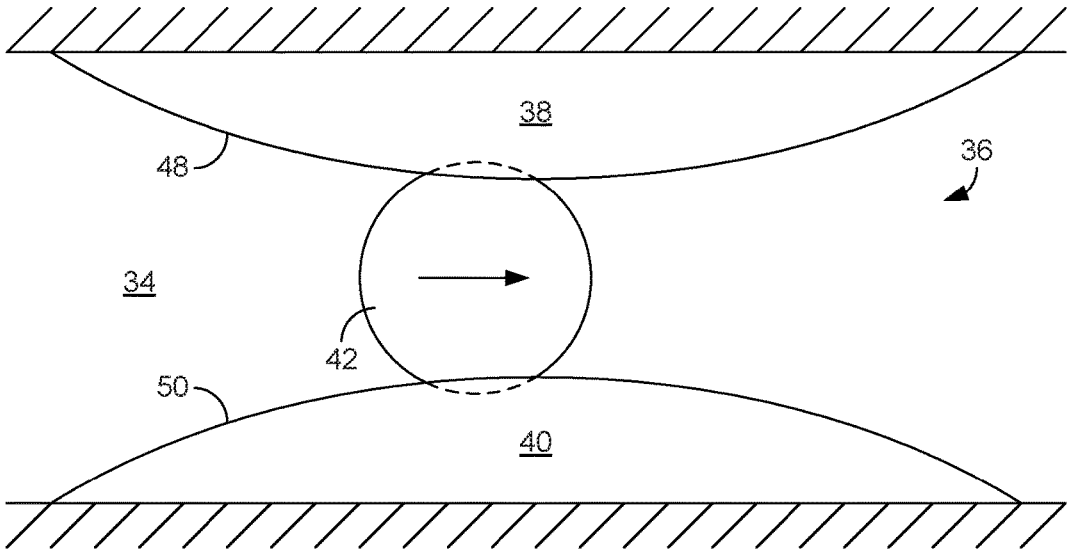

FIG. 2

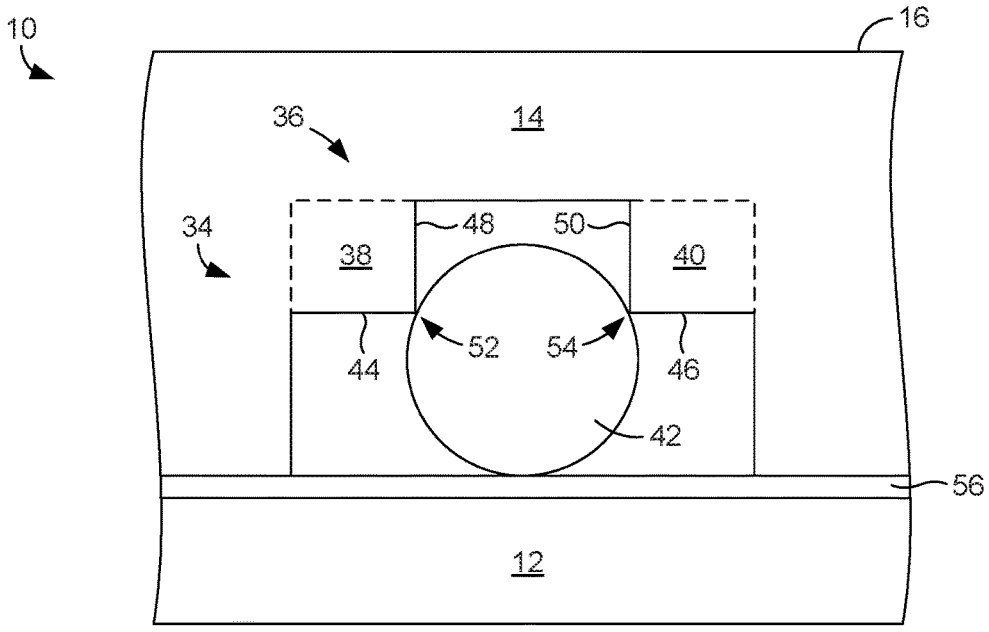

FIG. 3

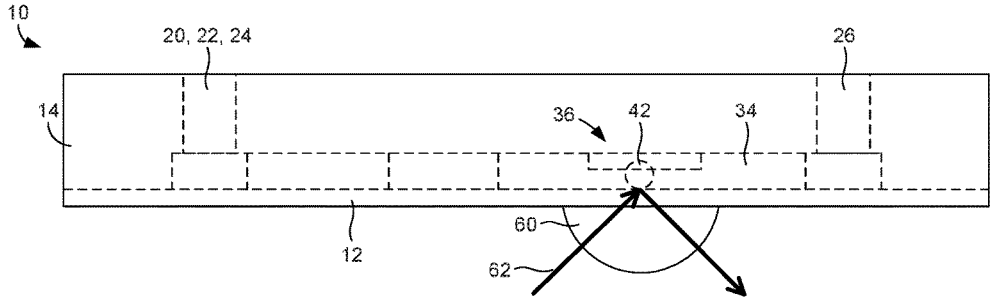

FIG. 4

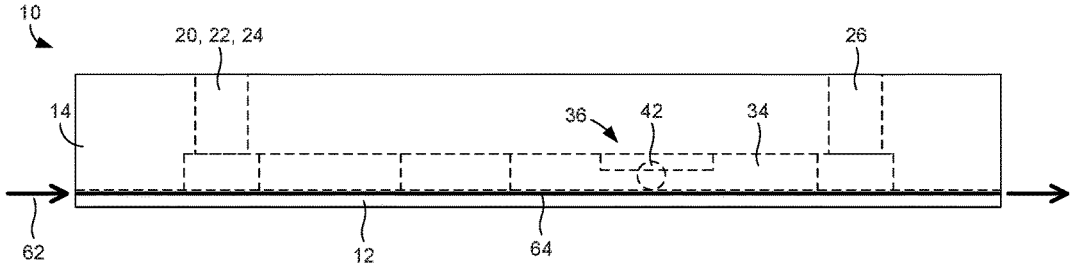

FIG. 5

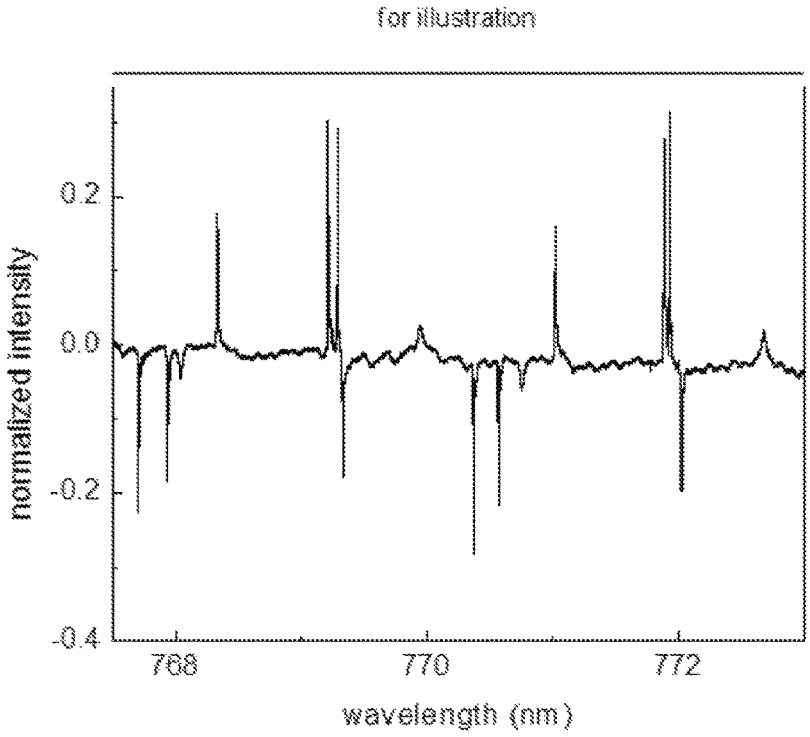
for illustration
normalized intensity
0.2
0.0
-0.2
-0.4
768
770
772
wavelength (nm)

FIG. 6

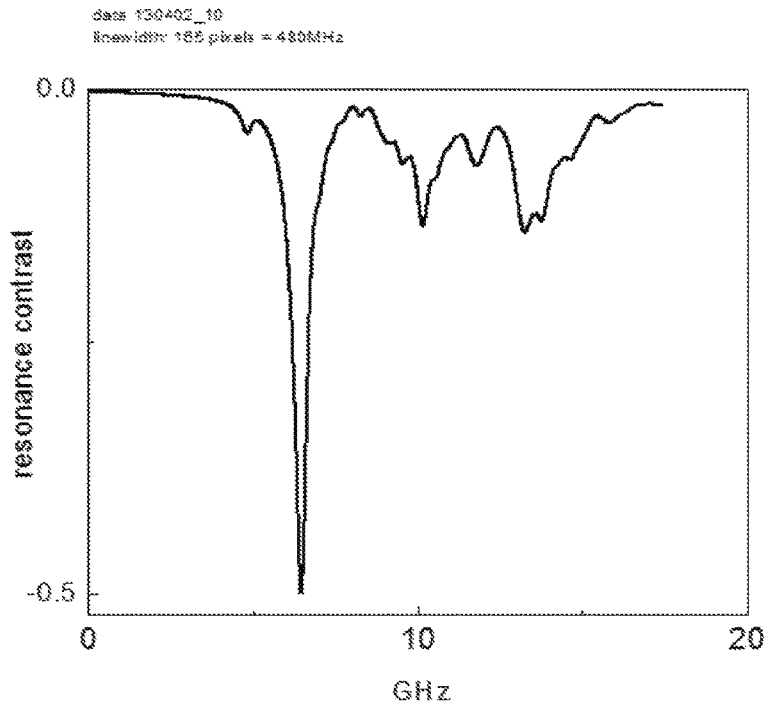
data 130402_10
linewidth: 165 pixels = 480MHz
0.0
-0.5
resonance contrast
0
10
20
GHz

FIG. 7

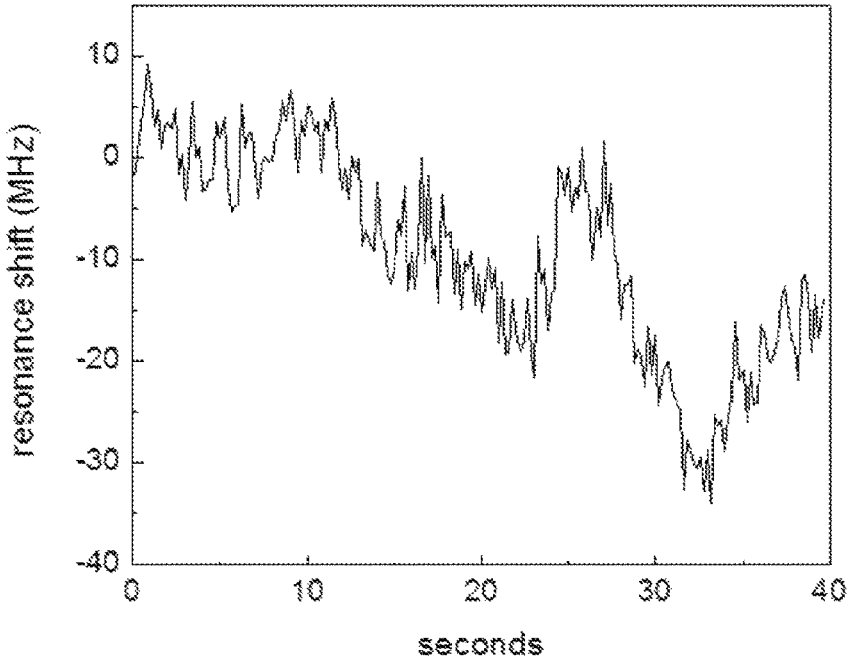
resonance shift (MHz)
10
0
-10
-20
-30
-40
0
10
20
30
40
seconds

FIG. 8

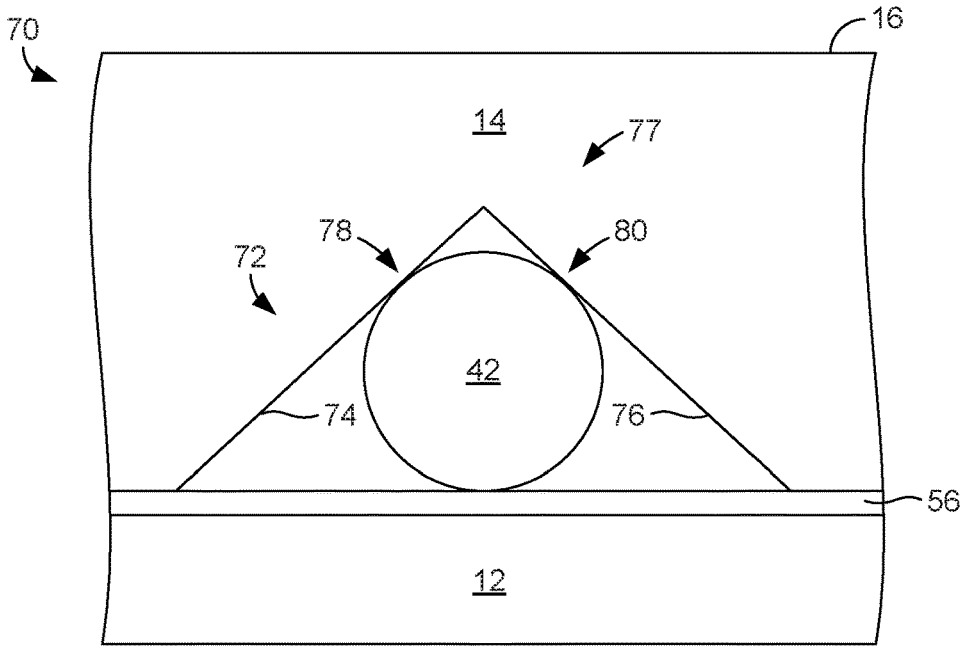
70
16
14
77
78
80
72
42
74
76
56
12

FIG. 9

MICROFLUIDIC PLATFORMS FOR OPTICAL BIOSENSING

CROSS-REFERENCE TO RELATED APPLICATION(S)

This application is a continuation application of U.S. Non-Provisional Application entitled "Microfluidic Platforms For Optical Biosensing," having Ser. No. 14/181,149 and filed Feb. 14, 2014, and claims priority to U.S. Provisional Application Ser. No. 61/764,298, filed Feb. 14, 2013, both of which are hereby incorporated by reference herein in their entireties.

BACKGROUND

Optical biosensors are powerful tools used in the analysis of biomolecular interactions, a key part of the drug discovery process. They can not only provide detailed information on the binding affinity and kinetics of the biomolecular interaction, but can also be exploited for the detection of bacteria and viruses for medical diagnosis, environmental monitoring, and homeland security.

A biosensor generally comprises a surface coated with biorecognition elements selected for their specific binding affinity with a molecule of interest (i.e., the molecule to be detected/measured). To be detected, binding must result in a physically detectable change. Optical biosensors are used to sense the local increase of refractive index that occurs near the surface as a result of the accumulation of the molecules of interest.

Optical resonator biosensors use optical resonators that exhibit sharp, i.e., high Q, optical resonances from their whispering gallery modes (WGM). Those resonances can be used for highly sensitive biodetection as they shift when small amounts of biomolecules attach to the resonator surface. As compared to planar devices, microresonator-based detectors take advantage of the recirculation of light, effectively increasing the interaction length with the sensing surface, thus yielding higher sensitivity.

Microsphere resonators made of dielectric material are particularly attractive because they can sustain high Q resonances and therefore provide more accurate results. In some cases, microspheres are placed on stems and are handled with micro-positioners. Unfortunately, it can be difficult to handle and position a microsphere in a desired manner in such circumstances because of the small size of the microsphere and the precision needed for its placement. In other cases, microspheres are permanently bonded to an optical substrate or fiber. While this can make it easier to handle and position the microsphere, such an arrangement is irreversible.

In view of the above discussion it can be appreciated that it would be desirable to have a way to easily handle and position a microsphere for optical biosensing.

BRIEF DESCRIPTION OF THE DRAWINGS

The present disclosure may be better understood with reference to the following figures. Matching reference numerals designate corresponding parts throughout the figures, which are not necessarily drawn to scale.

FIG. **1** is a perspective view of an embodiment of a microfluidic platform for positioning a microsphere for optical biosensing.

FIG. **2** is a schematic top view of a constriction of a primary channel of the microfluidic platform of FIG. **1**.

FIG. **3** is a cross-sectional view of the constriction shown in FIG. **2**.

FIG. **4** is a side view of the microfluidic platform of FIG. **1** illustrating a first method for performing optical detection.

FIG. **5** is a side view of the microfluidic platform of FIG. **1** illustrating a second method for performing optical detection.

FIG. **6** is a graph that shows a typical example resonance spectrum obtained from a 45 μm polystyrene (cross-linked with divinyl benzene) microsphere trapped in a fabricated microfluidic platform.

FIG. **7** is a graph that shows a resonance spectrum obtained using the fabricated microfluidic platform by performing a fine PZT wavelength scan over a selected resonance of mode number **1**.

FIG. **8** is a graph that shows a measured resonance frequency with a noise RMS of 10 MHz at a repetition rate of 5 Hz.

FIG. **9** is a cross-sectional view of a channel constriction of an alternative microfluidic platform.

DETAILED DESCRIPTION

As described above, it would be desirable to have a way to more easily handle and position microspheres for optical biosensing. Disclosed herein are microfluidic platforms that can be used for this purpose. In some embodiments, a microfluidic platform comprises a microfluidic channel through which a fluid that contains one or more microspheres can flow. The channel includes a constriction that can be used to trap a single microsphere in a position that facilitates optical biosensing. In some embodiments, the constriction makes three-point contact with the microsphere and leaves a top portion of the microsphere untouched.

In the following disclosure, various specific embodiments are described. It is to be understood that those embodiments are example implementations of the disclosed inventions and that alternative embodiments are possible. All such embodiments are intended to fall within the scope of this disclosure.

The present disclosure describes microfluidic platforms designed to position stand-alone microspheres at a precise location within a microfluidic channel of the platform. The platform is designed for ease-of-use and robustness and eliminates the need for optical alignment by an end user, while employing low-cost and disposable microspheres and removing the need for surface regeneration of the optical resonator.

FIG. **1** illustrates an example embodiment of a microfluidic platform **10**. As shown in this figure, the platform **10** generally comprises an optical substrate **12** on which is provided a top layer **14** that forms various channels of the platform. In some embodiments, the substrate **12** is made of a glass material having a thickness of approximately 900 to 1000 μm and an index of refraction of approximately 1.8 to 1.85. In some embodiments, the top layer **14** is made of a polymer material, such as polydimethylsiloxane (PDMS), and has a thickness of approximately 2000 to 3000 μm.

Multiple ports are formed in the top layer **14** that extend from a top surface **16** of the layer to a top surface **18** of the substrate **12**. In the illustrated embodiment, these ports include a microsphere inlet **20**, an analyte inlet **22**, a microsphere outlet **24**, and a multipurpose port **26**. The purpose for each of these ports is described below. In the illustrated embodiment, each of the microsphere inlet **20**, analyte inlet **22**, and microsphere outlet **24** are positioned at

a first end of the platform **10** and each is associated with an auxiliary channel **28**, **30**, and **32**.

The auxiliary channels **28**-**32** extend from their associated ports through the top layer **14** and along the substrate **12** to a primary channel **34** that extends to the multipurpose port **26** at the other end of the platform **10**. In some embodiments, the primary channel **34** is approximately 100 to 300 μm wide and 30 to 100 μm tall (e.g., 200 μm wide and 60 μm tall). As shown in FIG. **1**, the primary channel **34** includes a constriction **36** in a medial position along its length that can be used to trap microspheres (one at a time) for the purpose of performing optical biosensing.

FIGS. **2** and **3** illustrate the constriction **36** from top and end views, respectively. In the embodiment of FIGS. **2** and **3**, the constriction **36** has an inverted T-shaped cross section formed by two opposed inwardly-extending members **38** and **40** that gradually narrow a top portion of the primary channel **34** to a point at which a microsphere **42** can only travel along the channel to a specific position along the channel's length. In some embodiments, the inwardly-extending members **38**, **40** narrow the channel **34** to approximately 25 to 300 μm. As shown most clearly in FIG. **3**, the inwardly-extending members **38**, **40** can be defined by horizontal lower surfaces **44** and **46** and vertical upper surfaces **48** and **50** that define 90-degree edges **52** and **54** that contact opposite sides of the microsphere **42** at a point above its center. In such a case, the microsphere **42** can be securely held in place with three contact points including the two edges **52**, **54** and the substrate **12**. Because the locations at which the edges **52**, **54** contact the microsphere **42** only minimally overlap the excited optical mode of the microsphere, which is confined to a region near the vertical equatorial plane of the microsphere, the edges do not affect the Q-factor of the whispering gallery mode resonances.

As is further shown in FIG. **3**, the surface **18** of the substrate **12** can comprise a low-index separation coating **56**. In some embodiments, this coating **56** is approximately 400 nm to 600 nm thick. When the separation coating **56** is present, the microsphere **42** contacts the separation coating, which optimizes coupling of light to the microsphere. The separation coating **56** can be made of a polymeric material having an index of refraction that matches that of a liquid (e.g., water) that is used with the platform **10**. In some embodiments, the separation coating **56** has an index refraction of approximately 1.33 to 1.35, which is close to the refractive index of water. By way of example, the separation coating **56** can be made of an amorphous fluoropolymer, such as Cytop®, which is available from Bellex International, Corp.

When the platform **10** is to be used for optical biosensing, a liquid (e.g., water) that contains one or more microspheres that is/are coated with suitable biorecognition elements can be delivered to the auxiliary channel **28** via the microsphere inlet **20**. If the analyte inlet **22** and the microsphere outlet **24** are both closed, the liquid will flow through the primary channel **34** to the multipurpose port **26** through which the liquid can exit the platform **10**. Because of the constriction **36** in the primary channel **34**, however, a microsphere that travels along the primary channel **34** because of the liquid flow will become trapped by the constriction at a location at which light can be coupled with the microsphere during optical biosensing. If the liquid contains other microspheres and the clearing of those microspheres is desired, the microsphere inlet **20** can be closed, the microsphere outlet **24** can be opened, and liquid can be delivered to the primary channel **34** via the multipurpose port **26**. If the flow is gentle, the trapped microsphere will remain trapped in the constriction **36**, but any other microspheres in the platform **10** will be removed via the auxiliary channel **32** and the microsphere outlet **24**.

At this point, the microsphere outlet **24** can be closed and an analyte fluid that comprises molecules that will bind with the biorecognition elements on the surface of the microsphere can be delivered to the primary channel **34** via the analyte inlet **22** and the auxiliary channel **30**. Optical biosensing can be simultaneously performed to determine whether or not the molecules have bound to the microsphere and, if so, to what degree. FIGS. **4** and **5** illustrate two example optical biosensing approaches.

Once the optical biosensing has been completed, the microsphere outlet **24** can be again opened and the contents of the platform **10** can be flushed by delivering fluid through the multipurpose port **26**. If the flow is strong enough, the trapped microsphere will dislodge from the constriction **36** and exit the platform **10** via the microsphere outlet **24**. Accordingly, the platform **10** can be described as a trap-and-release microfluidic platform.

As mentioned above, FIGS. **4** and **5** illustrate example methods for performing optical biosensing with the platform **10**. Beginning with FIG. **4**, optical measurements can be performed using a hemispherical prism **60** by frustrated total internal reflection. In such a case, a beam of light **62** can be directed through the hemispherical prism **60** from below the platform to enable the light to couple with the microsphere **42**. In FIG. **5**, the microsphere **42** is addressed using an optical waveguide **64** that is constructed on top of the substrate **12**.

The microsphere used in the microfluidic platform can be made of one or more of a variety of different dielectric materials. Example materials include polystyrene and silica. The size of the microsphere, and therefore the primary channel and its constriction, can vary depending upon the particular application and microsphere material. In some embodiments, the microsphere has a diameter of approximately 25 to 500 μm.

In some embodiments, the microsphere is a polystyrene microsphere having a diameter of approximately 30 to 45 μm. Such microspheres exhibit sharp resonances and therefore hold great promise for highly sensitive biosensing. These microspheres can be surface modified for affinity-based assays. Polystyrene microspheres (cross-linked with divinylbenzene) with diameters of 45 μm have already shown a good potential for biosensing with whispering gallery mode (WGM) resonances of Q-factor in excess of 10^6 and a demonstrated detection limit of 1.5×10^{-6} RIU, equivalent to a surface coverage of 0.7 pg/mm^2. The detection limit was mostly attributed to frequency jittering of the scanning laser of about 7 MHz, while the contribution of intensity noise in the data is merely 300 kHz, corresponding to a detection limit of 0.023 pg/mm^2.

As indicated in Table 1, both the Q-factors and sensitivities of 45 μm spheres are on par with the most sensitive measurements reported with a 70 μm silica sphere with a detection limit of 0.028 pg/mm^2. However, in the latter case, substantial efforts were made to improve the stability of readily available commercial lasers by frequency doubling of a 1300 nm DFB laser. It was therefore possible to fit the position of the Lorentzian peak with a precision on the order of 460 kHz. With a laser of similar stability, the same detection limit in terms of surface coverage per unit area can be achieved with 45 μm polystyrene spheres. It should be noted that the frequency doubling technique used by Shopova et al. has the disadvantage of reducing the wavelength scanning range to just 0.1 nm, which is less than the

free spectral range of the optical resonators. As a consequence, only a few of the fabricated spheres would have sharp resonances that lie in the accessible spectral range because of the inherent size variations limited by the fabrication tolerance (for all types of resonators listed).

TABLE 1

Optical resonator biosensors that have demonstrated the best detection limit.

Technology	Reference	Loaded Q in water	sensitivity (shift in pm per pg/mm^2)	noise detection limit, bulk R1 sensing	noise detection limit, surface coverage	single particle detection noise limit
OFFR microtoroid, silica	[15] [14]	1.2×10^5 10^8	0.145	4×10^{-8}	0.14 pg/mm^2	InfA virus 38:1 SNR- 13 ag DL
microsphere, silica, 300 μm	[10]	2×10^6	0.011		15 pg/mm^2	
microsphere, silica, 70 μm	[17]	10^6	0.023	4.5×10^{-8}	0.28 pg/mm^2	InfA virus 26:1 SNR- 20 ag DL
microsphere, polystyrene	[19]	10^6	0.02	1.5×10^{-6}	0.71 pg/mm^2 4.5 fg	

Because of their smaller size, 45 μm polystyrene spheres are more sensitive than 70 μm silica spheres to single particles binding at the equator, with respective shifts of 29 fm and 15 fm calculated for a single InfA virus. By further reducing the polystyrene sphere diameter from 45 μm to 25 μm, which should not affect the Q-factor, it is anticipated that the sensitivity per uniform mass coverage per unit area would be improved by two-fold, while increasing the shift associated with a single particle binding at the equator by a factor of 5 at 160 fm. Hence, a ten-fold improvement in the detection limit would be expected as compared to the work by Shopova et al. for a single particle binding at the equator, provided a laser system of similar stability is utilized.

The laser used for the optical biosensing can, in some embodiments, have a lesser stability of about 1-4 MHz when repetitively scanned over the resonance, yielding a detection limit of about 0.05 to 0.2 pg/mm^2 for 25 μm polystyrene microspheres. By using 25 μm polystyrene spheres, a single particle mass detection limit of 20 ag should be achievable, which is close to the best detection limit ever reported in the range of 13 ag, with the added benefit of using commercially-available tunable lasers together with low-cost and disposable stand-alone microspheres in a reusable microfluidic cell.

Microspheres made from other types of materials such as melamine and silica are also available. Some manufacturers offer microspheres made from custom monomers. Perfluorinated polymer microspheres may be of special interest because of their low material loss and may therefore hold great promise for obtaining higher Q.

A microfluidic platform having the configuration described above was fabricated for testing purposes. During the fabrication, the various channels of the platform were formed in a layer of PDMS using soft lithography. In this process, a mold was first fabricated out of SU-8 resist by photolithography on silicon. Two layers of SU-8 were used with double exposure and single development in order to define the inverted T-shape cross-section of the primary channel. PDMS was then poured onto the mold, baked, and released. The PDMS layer was then bonding to the optical substrate, which comprised a medium refractive index glass (1.41) having a spin-coated, 580 nm thick coating of Cytop® with refractive index of 1.34 to optimize optical coupling to the trapped sphere. In essence, this allows the microsphere to behave as if it is entirely surrounded by water.

The platform was tested to evaluate its trap-and-release functionality. This testing confirmed that the microsphere can be securely trapped so that, if excess microspheres accumulate, they can be flushed from the platform with gentle flow of liquid in the opposite direction without dislodging the trapped microsphere. A much stronger flow, however, was observed to release the trapped microsphere.

The WGM resonances of the microspheres were measured through the optical substrate by frustrated total internal reflection, which occurred at the interface between the high refractive index glass (1.84) and Cytop® (1.34, i.e. close to the refractive index of water). The optical set up was similar to what was reported in "High Q Optical Resonances of Polystyrene Microspheres in Water Controlled by Optical Tweezers", Applied Physics Letters, 2007, 91: p. 14116, by Lutti et al., which is hereby incorporated by reference in its entirety, with exception of the light source, which was an externally tunable diode laser (TL 6712 Velocity) emitting around 780 nm. This enabled spectral scanning without mode hopping over several free spectral ranges using motor tuning and fine scanning over a resonance using lead zirconate titanate (PZT) scanning.

The optical substrate was placed in contact with an index-matching cut ball lens that formed a hemispherical lens. The laser light was focused to a 4 μm spot at the glass-Cytop® interface with an angle of incidence of approximately 54°, i.e. in the total internal reflection regime, thus creating an evanescently decaying electromagnetic (EM) field in the Cytop® coating and water. When a microsphere was immobilized on the Cytop® surface in spatial overlap with the evanescent field, light could be coupled to the microsphere WGM at resonant frequencies, decreasing the reflected intensity. Resonance spectra were obtained by scanning the laser frequency over one or several resonances. The spot size and angle of incidence were chosen to optimize coupling to the WGMs from calculation

and by experimental tuning. Both horizontal (x) and vertical (y) polarizations, which couple respectively to the transverse-magnetic (TM) and transverse-electric (TE) WGMs, were simultaneously measured by rotating the light polarization to about 45°. Because resonant frequencies are different in each polarization, one polarization can serve as a reference for light intensity when measuring resonances in the other, thus eliminating noise due to light intensity fluctuations. Hence, detection uses two photodiodes and an oscilloscope to measure the difference between the vertically and horizontally polarized reflected intensities. The WGMs in the TE and TM polarizations, respectively, appear as dips and peaks in the reflectivity spectrum obtained by scanning the laser frequency.

It is noted that the positions of the three contact points of the channel constriction preserve the integrity of the optical modes. In the case of a perfectly spherical microresonator, the resonator modes are degenerate and all modes with the same azimuthal number have the same frequency. Evanescently coupling light to the resonator at the resonant frequency by Fourier transform infrared spectroscopy (FTIR) through a prism or by coupling through a fiber excites a subset of those modes, which are in spatial overlap with the excitation. If mode matching is satisfied, then the preferentially excited mode is the equatorial mode, for which the EM field is primarily distributed around a narrow band near the equatorial plane of the sphere in the plane of incidence. When the resonator departs for perfect sphericity, the degeneracy is lifted, with the arising of several resonant frequencies that correspond to modes being various mixes of the azimuthal modes. Even in cases in which the asphericity is not known or controlled, it is more likely that the modes that can be most strongly excited via evanescent coupling with the same mode matching condition are those that have the highest content of the equatorial modes. Therefore, it is desirable that the equator does not overlap with scattering elements such as PDMS contact points, which would decrease the high Q of the resonances.

FIG. **6** shows a typical example of a resonance spectrum obtained from a 45 μm polystyrene (cross-linked with divinyl benzene) microsphere trapped in the platform in water. The microspheres were purchased from Polysciences, Inc. The spectrum was obtained by scanning the laser wavelength using coarse motor tuning while recording the intensity reflected at the Cytop®/glass interface, as described earlier. The spectrum was calibrated using the intensity measured in the TE polarization only in the absence of a microsphere, so that an amplitude of −1 corresponds to complete extinction in the TE (resp. TM) polarization. This scan enables one to locate the resonances and determine the microsphere diameter by comparison with theory, which was determined as 45.8±0.2 μm for this microsphere.

FIG. **7** shows a resonance spectrum obtained by performing a fine PZT wavelength scan over a selected resonance of mode number **1**. Using a Lorentzian line shape, the full width at half maximum (FWHM) of the main peak was 480 MHz, corresponding to a Q-factor of 0.8×10^6, which is a typical value for the microspheres that we have measured. This is consistent with typical Q-factors previously measured for the same type of microspheres while they were held at a distance from the substrate by optical tweezers, showing that the trapping method did not significantly decrease the optical mode quality. For this measurement, the center wavelength of the resonance was measured with a noise RMS of 10 MHz at a repetition rate of 5 Hz, limited by repeatability of the laser wavelength scan (FIG. **8**). This translated into 1.0 pg/mm^2 for biosensing application.

Although a particular constriction geometry has been illustrated and described above, it is noted that alternative geometries can be used to trap and release microspheres. FIG. **9** illustrates an example of an alternative geometry. In this embodiment, a primary channel **72** of a platform **70** has a triangular cross-section formed by opposing walls **74** and **76** that form a constriction **77**. The walls **74**, **76** contact the microsphere **42** at opposing points **78** and **80** on opposite sides of the microsphere. Like the constriction **36** of the first embodiment, the constriction **77** does not contact the top of the microsphere **42** and therefore only minimally overlaps the excited optical mode of the microsphere.

The invention claimed is:

1. A microfluidic platform for optical biosensing, the platform comprising:

an optical substrate;

a layer provided on the optical substrate; and

a channel formed within the layer and defined by the layer and the optical substrate through which fluid can flow, the channel including a channel constriction defined by a surface of the optical substrate and two opposed inwardly-extending members of the layer that extend inward from opposed lateral sides of the channel in a manner in which they gradually narrow[s] a width of the channel along its length to a point at which the channel is physically sized and configured to trap a microsphere suspended in the fluid when the fluid flows through the channel, wherein the optical substrate surface and the two opposed members together form three separate contact points of the channel constriction that are configured to contact the microsphere at three different points without any part of the channel contacting a top of the microsphere.

2. The platform of claim **1**, wherein the channel at the channel constriction has an inverted T-shape in cross-section.

3. The platform of claim, **1** wherein the inwardly-extending members are defined by lower surfaces and upper surfaces that form opposing edges that contact opposite sides of the microsphere.

4. The platform of claim **3**, wherein the lower surfaces are horizontal, the upper surfaces are vertical, and the edges are 90-degree edges.

5. The platform of claim **1**, wherein the channel at the channel constriction has a triangular cross-section and the opposed inwardly-extending members comprise opposing walls of the layer that are angled toward each other.

6. The platform of claim **1**, further comprising multiple ports formed in the layer that provide access to the channel.

7. The platform of claim **6**, wherein there are multiple ports provided at a first end of the platform that provide access to a first end of the channel and a port provided at a second end of the platform that provides access to a second end of the channel.

8. The platform of claim **7**, wherein the channel is a primary channel and further comprising auxiliary channels that extend from the multiple ports at the first end of the platform to the primary channel.

9. The platform of claim **1**, further comprising a separation coating provided on the optical substrate and contacting the layer.

10. A microfluidic channel for trapping a microsphere, the channel comprising:

a channel constriction that gradually narrows in width along a length of the channel to a point at which the channel is physically sized and configured to trap a microsphere having a diameter of approximately 20 to

500 microns that is suspended in a fluid when the fluid flows through the channel, wherein the channel constriction comprises a bottom surface and two opposed inwardly-extending members that extend inward from opposed lateral sides of the channel, wherein the bottom surface and the two opposed inwardly-extending members together form three contact points that are configured to contact the microsphere at three different points without any part of the channel contacting a top of the microsphere.

11. The channel of claim **10**, wherein the channel at the channel constriction has an inverted T-shape.

12. The channel of claim **10**, wherein the inwardly-extending members are defined by lower surfaces and upper surfaces that form edges that contact opposite sides of the microsphere.

13. The channel of claim **12**, wherein the lower surfaces are horizontal, the upper surfaces are vertical, and the edges are 90-degree edges.

14. The channel of claim **10**, wherein the channel at the channel constriction has a triangular cross-section and the opposed inwardly-extending members comprise opposing walls of the layer that are angled toward each other.

* * * * *